Chemistry & Biology
Article

Determining the Structure and Mode of Action of Microbisporicin, a Potent Lantibiotic Active Against Multiresistant Pathogens

Franca Castiglione,[1] Ameriga Lazzarini,[1] Lucia Carrano,[1] Emiliana Corti,[1] Ismaela Ciciliato,[1] Luciano Gastaldo,[1] Paolo Candiani,[1] Daniele Losi,[1] Flavia Marinelli,[2,*] Enrico Selva,[1] and Francesco Parenti[1]
[1]Vicuron Pharmaceuticals, Via R. Lepetit 34, 21040 Gerenzano, Varese, Italy
[2]DBSM, University of Insubria, Via J.H. Dunant 3, 21100, Varese, Italy
*Correspondence: flavia.marinelli@uninsubria.it
DOI 10.1016/j.chembiol.2007.11.009

SUMMARY

Antibiotics blocking bacterial cell wall assembly (β-lactams and glycopeptides) are facing a challenge from the progressive spread of resistant pathogens. Lantibiotics are promising candidates to alleviate this problem. Microbisporicin, the most potent antibacterial among known comparable lantibiotics, was discovered during a screening applied to uncommon actinomycetes. It is produced by *Microbispora* sp. as two similarly active and structurally related polypeptides (A1, 2246-Da and A2, 2230-Da) of 24 amino acids linked by 5 intramolecular thioether bridges. Microbisporicin contains two posttranslational modifications that have never been reported previously in lantibiotics: 5-chloro-trypthopan and mono- (in A2) or bis-hydroxylated (in A1) proline. Consistent with screening criteria, microbisporicin selectively blocks peptidoglycan biosynthesis, causing cytoplasmic UDP-linked precursor accumulation. Considering its spectrum of activity and its efficacy in vivo, microbisporicin represents a promising antibiotic to treat emerging infections.

INTRODUCTION

Infections caused by Gram-positive pathogens constitute a major burden on patients and healthcare systems globally. This scenario is further complicated by the emergence of resistant strains no longer predictably susceptible to standard first-line antimicrobials, such as oxacillin or vancomycin (Johnson and Woodford, 2002). In particular, methicillin-resistant *Staphylococcus aureus* (MRSA) strains are often multiresistant to several antibiotic classes. They represent the major cause of serious infections acquired in the hospital, and have recently emerged in communities. This has resulted in the wide use of glycopeptides, such as vancomycin and teicoplanin, as drugs of last resort for serious MRSA infections. However, glycopeptide tolerance has now emerged, too, and highly vancomycin-resistant clinical *S. aureus* (VRSA) isolates have recently been described (Johnson and Woodford, 2002; Appelbaum, 2006). Medical need is driving the search for novel, and more effective antibiotics against MRSA, and hopefully also for treating other clinically important Gram-positive pathogens. In this context, we recently devised a screening strategy for identifying inhibitors of bacterial cell wall biosynthesis, different from β-lactams and glycopeptides, and thus potentially capable of overcoming existing resistance mechanisms (Castiglione et al., 2007).

The screening was applied to the Vicuron library of 120,000 broth extracts obtained by fermenting 40,000 uncommon actinomycetes isolated in the environment (Castiglione et al., 2007; Lazzarini et al., 2001). The primary assay was devised to identify microbial extracts containing peptidoglycan (PG) biosynthesis inhibitors on the basis of their differential activity against *S. aureus* and its L form (Castiglione et al., 2007; Somma et al., 1977). Secondary selection was oriented to discard those extracts containing β-lactams or glycopeptides. It was based on whether antimicrobial activity against *S. aureus* could be reversed by a β-lactamase cocktail or by adding D-Ala-D-Ala affinity resin (Corti et al., 1985). Through this approach, five novel lantibiotics were identified. In this paper, we report on the structure elucidation and biological profiling of the most potent among these novel lantibiotics, named microbisporicin. Its structure is original, containing two posttranslational modifications that have not been reported previously in lantibiotics. Microbisporicin's antimicrobial activity is superior to comparable, known lantibiotics.

Lantibiotics are ribosomally synthesized and posttranslationally modified peptides produced by Gram-positive bacteria (Jung, 1991). They contain thioether intramolecular cross-linked amino acids, termed lanthionines (Lans) or 3-methyllanthionines (Melans), in addition to the unsaturated amino acids, 2,3-didehydroalanine (Dha) and (Z)-2,3-didehydrobutyrine (Dhb) (Chatterjee et al., 2005; Cotter et al., 2005; Pag and Sahl, 2002). Traditionally, these peptides have been classified, on the basis of structural and functional aspects, as being either type A or type B lantibiotics. Nisin, which has been used in the dairy industry for over 40 years, was considered the prototype for the flexible amphiphilic type A lantibiotics, which act by forming pores in the cell membrane of susceptible cells (Jung, 1991). It is a 3353 Da cationic, elongated peptide, 34 amino acids long, containing five intramolecular ring structures, which is produced by *Lactococcus lactis* sub *lactis* (Jung, 1991; Chatterjee et al., 2005; Pag and Sahl, 2002). In contrast, type B lantibiotics, such as mersacidin (Chatterjee et al., 1992), actagardine (Somma et al.,

1977; Parenti et al., 1976), and cinnamycin (Machaidze and Seelig, 2003), are more globular and compact in structure, and act by inhibiting the function of various enzymes by binding to membrane lipids. Mersacidin (1825 Da) (Chatterjee et al., 1992) and actagardine (also termed gardimycin) (1890 Da) (Somma et al., 1977; Parenti et al., 1976) are structurally similar tetracyclic hydrophobic peptides, 20 and 19 residues long, containing four intramolecular thioether rings, which are produced by a *Bacillus* strain and by an *Actinoplanes* species, respectively. They inhibit PG synthesis by binding to lipid II, the essential membrane-bound precursor for cell wall formation (Brotz et al., 1998a). Cinnamycin-like peptides, 19 amino acids long, produced by *Streptomyces* spp. show distinct functions, inhibiting phospholipases by binding phosphatidylethanolamine (Machaidze and Seelig, 2003). However, the distinction between type A and type B lantibiotics has become blurred, as it was observed that nisin interacts in a highly specific manner with lipid II (Breukink et al., 1999). Lipid II, indeed, acts as a docking molecule for nisin, and energetically facilitates the formation of membrane pores (Breukink et al., 1999; Hasper et al., 2006). A more recent classification of lantibiotics in different subgroups has been proposed based on the organization of their biosynthetic genes and enzymes, rather than on the activity profile or three-dimensional structure (Chatterjee et al., 2005; Cotter et al., 2005).

The renewed interest in the chemotherapeutic potential of antibacterial lantibiotics that inhibit cell wall synthesis originates from the fact that they are effective in treating infections sustained by MRSA and that they did not show cross-resistance with glycopeptides (Castiglione et al., 2007; Cotter et al., 2005). In fact, their complex with lipid II differs greatly from the glycopeptides-lipid II complex, and does not involve the C-terminal D-alanyl-D-alanine (D-Ala-D-Ala) moiety of the pentapeptide side chain of the lipid intermediate, but, rather, equally blocks access of the transglycosylase to its substrate (Brotz et al., 1997, 1998a). In this light, microbisporicin discovery may provide additional insights into the molecular determinants of the biological activity of lipid II-targeting antibiotics.

RESULTS

Identification, Production, and Purification of Microbisporicin

Microbisporicin, previously patented as antibiotic 107891 (Lazzarini et al., 2005), was discovered during the screening approach described elsewhere (Castiglione et al., 2007), which was applied to the Vicuron collection and devised to target novel PG biosynthesis inhibitors. The microbisporicin-containing microbial extract was found to be at least 8-fold more active against *S. aureus* than against its L form and insensitive to the addition of a β-lactamase cocktail or D-Ala-D-Ala affinity resin, according to the primary and secondary screening criteria (data not shown). It is produced by the actinomycete, *Microbispora* ATCC PTA-5024, as two factors (microbisporicin A1 and A2), typically in a 60:40 ratio (see Experimental Procedures for the fermentation and purification conditions). The antibiotic was found either in the supernatant of the harvested broth or associated with the mycelium, with a total estimated productivity ranging from 10 to 20 mg/l of culture. It was purified by multistep chromatography. Microbisporicin remained substantially stable during the purification process. Its stability was checked in methanolic extracts containing 0.1–0.5 mg/ml of the antibiotic, at different pH values (3, 6, 7.5, and 9.5) and temperatures (4 and 40°C). The antibiotic half-life at 40°C was more than 1 month in the 2–6 pH range, decreasing progressively at pHs from 6 to 7.5. At pH 9.5, the half-life was approximately 1 week at 4°C and 1 day at 40°C, respectively.

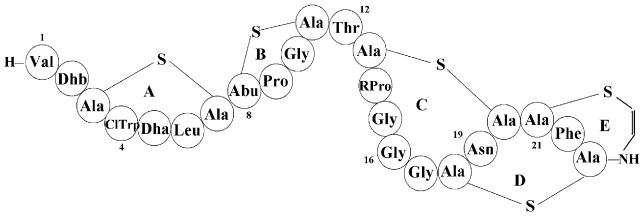

RPro = 3,4-dihydroxy-proline in A1
RPro = 4-hydroxy-proline in A2

Figure 1. Primary Structure of the Antibiotic Microbisporicin A1 and A2

Structure Determination of Microbisporicin A1 and A2

The structures assigned to microbisporicin A1 and A2 (Figure 1) have been elucidated by spectroscopic and degradation studies. The investigation focused first on microbisporicin A2. The ^{1}H NMR spectrum reflected a pattern typical for small peptide molecules. The amino acid spin systems were identified and assigned by analyzing double-quantum filtered correlation spectroscopy (DQF-COSY) and total correlation spectroscopy (TOCSY) experiments, as described by Bax and Davis (1985) and Griesinger et al. (1988). Table 1 reports the proton chemical shifts of the individual amino acids, together with their CHα-NH coupling constants and amide proton temperature coefficients. The experiments revealed that five proteinogenic amino acid spin systems, Val, Leu, Pro, Asn, and Thr, occur only once. Gly spin system appeared four times, and a 4-hydroxy-proline (4-OHPro) was identified. Two aromatic ring systems were assigned by examining the aromatic region of the DQF-COSY spectrum. Some doublets and triplets, corresponding, respectively, to a chloro-tryptophan (ClTrp) residue and to phenylalanine (Phe), were observed. As there was no mutual coupling, connectivities between the aromatic protons and their backbone protons could only be established through nuclear Overhauser enhancement (NOE) spectroscopy (NOESY) experiments. In addition, spin systems of some amino acids, characteristic of lantibiotics, were present. Dha, Dhb, and 2-aminovinyl-cysteine (AviCys) were found in the characteristic spectral region of 5.5–7.0 ppm (Wishart and Nip, 1998). Finally, the α-aminobutyric acid (Abu) part of the Melan unit appeared once, whereas three Lans (Ala-S-Ala) were identified. A majority of amide protons were observed and assigned to the corresponding CHα, as reported in Table 1.

To assign the peptide sequence, we investigated short-range NOESY crosspeaks between the CHα, CHβ, or amide proton of (*i*) residue and the amide proton of the adjacent (*i* + *1*) residue in the peptide sequence (Wüthrich, 1986), denoted by αN, βN, and NN, respectively. In microbisporicin A2, a sequence of such NOEs could be traced for the majority of the 24 amino acid

Table 1. Proton Chemical Shifts of the Individual Amino Acids Constituting Antibiotic Microbisporicin A2 Together with Their J Coupling Constants and Amide Temperature Coefficients

Residue	NH (ppm)	CHα (ppm)	CHβ (ppm)	Others (ppm)	J (NH-CHα) (Hz)	Δδ/T (−ppbK^{-1})
Val1	—	3.94	2.27	Me: 1.06–1.08		—
Dhb2	—	—	6.39	Me: 1.79		—
Ala3	7.86	4.62	3.25–2.94		5	10
ClTrp4	8.23	4.6	3.31–2.93	7.03,7.15,7.33,7.48, 10.4	7.7	6
Dha5	—	—	5.54–6.04			
Leu6	8.68	4.18	1.7–1.73	Me: 0.92–0.98; CHγ: 1.63		8
Ala7	8.04	4.58	2.92–3.07			5.2
Abu8	8.31	—	3.36	Me: 1.17	10.2	4.2
Pro9	—	4.33	2.39–1.8	CHγ: 1.83–2.07; CHδ: 3.0–3.46		—
Gly10	8.44	4.36–3.52				4
Ala11	7.68	4.03	2.92–3.62			4
Thr12	8.1	4.18	4.39	Me: 1.3	5.2	8
Ala13	9.25	4.24	2.99–3.49			4
4-OHPro14	—	4.54	2.37–1.93	CHδ: 3.6–3.86		—
Gly15	7.68	3.68–4.13				4.1
Gly16	8.49	3.39–4.29				3.3
Gly17	8.04	3.98–4.38				2.9
Ala18	8.68	4.43	3.26			8.1
Asn19	9.39	4.43	2.79–3.02	NH_2γ: 6.79–7.55		8
Ala20	8.89	4.19	3.11–3.81			10
Ala21	7.99	4.99	2.98–3.13		8.9	2.2
Phe22	9.78	4.3	3.3–2.98	7.23, 7.36		10
Ala23	9.34	4.15	2.64–3.43			2
Avi24	8.58	6.93	5.64		10.2	

Microbisporicin A2 was dissolved in H_2O/MeOH-d3 at 300K.

residues of the structure shown in Figure 1. The C-terminal sequence Avi24-Ala23-Phe22-Ala21 was established with the assigned low-field amide protons at 9.78 ppm (Phe22), 9.39 ppm (Asn20), and 9.34 ppm (Ala23); beginning with the Avi24 residue, four interresidue NOESY peaks with Ala21, Ala23, and Phe22 were found. Moreover, correlations between NH Avi24-CHα Ala23, NH Ala23-CHα Phe22, and NH Phe22-CHα Ala21 were identified. The sulfide ring E was elucidated on the basis of the correlation between CHβ Avi24 and CHβ Ala21. The Avi24-Ala21 bridge was also consistent with NOE and long-range connectivities found between Avi24Hβ and Ala21Hβ protons. Similarly, it was possible to sequentially assign the rest of the molecule by using the information from NOESY spectra acquired at 313K and 293K, together with the heteronuclear multiple bond correlation (HMBC) data. The position of the sulfide bridges could also be deduced from ^{13}C-^{1}H multiple-bond correlations C-S-C-H between the two amino acids forming the bridge and then confirmed by NOE crosspeaks between β-protons in the Ala residues of the Lan. In microbisporicin A2, the connectivities Ala3-Ala7, Ala13-Ala20, Ala18-Ala23, and Abu8-Ala11 were observed in this way. The complete set of interresidue NOE data are listed in Table S1 in the Supplemental Data available with this article online. The carbon chemical shifts of all amino acid residues are listed in Table 2. The ^{13}C resonances of all the carbons could be assigned without overlap by using the heteronuclear multiquantum correlation (HMQC) and HMBC spectra. A similar experimental approach was followed to determine the structure of microbisporicin A1. In this case, twin spin systems for all the amino acids were present due to a slow conformational equilibrium observed in solution. Notwithstanding the increased spectral complexity, proton chemical shifts and the CHα-NH coupling constants were established for the individual amino acids, as reported in Table S2. Interresidue NOE data are listed in Table S3 of the Supplemental Data. Microbisporicin A1 and A2 differed only in the amino acid residue in position 14. A 3,4-dihydroxy-proline (3,4-diOHPro) residue was found in microbisporicin A1 in place of 4-OHPro in A2 (Figure 1).

Mass spectrometry (MS) analyses were performed on the hydrolyzed and intact antibiotic to further confirm the structure assigned by NMR. The liquid chromatography (LC)-MS analysis of the acidic hydrolysis mixture showed the presence of the Lan, Melan, Gly, Thr, Pro, Val, Phe, Leu, and Asp amino acids, the last derived from Asn residue under the strong acidic conditions applied for the hydrolysis. The residues Dha, Dhb, ClTrp, and AviCys were not found, probably because of their instability under these conditions. The peculiar 5-ClTrp was identified when either A1 or A2 was hydrolyzed by using a protocol that prevented its acidic degradation (Simpson et al., 1976). It coeluted with an authentic standard at 11.5 minutes and showed

Table 2. ^{13}C Chemical Shift of the Individual Amino Acids Constituting the Antibiotic Microbisporicin A2 in D_2O/CH_3CN-d3 at 313K

Residue	CO (ppm)	Cα (ppm)	Cβ (ppm)	Cγ (ppm)	Others (ppm)
Val1	170	59.5	30.95		Me: 17.89, 18.72
Dhb2	165.7	129.2	132.9		Me: 13.6
Ala3		54.45	37.6		
ClTrp4		56.87	27.4		**2**) 126.8; **3**) 109.7; **4**) 118.6; **5**) 124.9; **6**) 122.4; **7**) 113.8; **8**) 135.6; **9**) 129.1
Dha5	167.1	134.8	106.7		
Leu6		54.14	40.2	25.6	Me: 21.9, 22.9
Ala7		56.8	35.2		
Abu8		57.92	49.77		Me: 21.9
Pro9	—	61.79	29.36	26.84	CHδ: 49.22
Gly10		43			
Ala11		55.8	37.1		
Thr12		59.72	68.53		Me: 20.12
Ala13		—	37.3		
4-OHPro14	—	64.71	37.39	70.71	CHδ: 56.74
Gly15		43.3			
Gly16		43.3			
Gly17		43.5			
Ala18		54	34.5		
Asn19		54.5	35		
Ala20		—	36		
Ala21		54.5	32.74		
Phe22		60.45	37.86		137.3; **2**) 129.7; **3**) 130.1; **4**) 128.1
Ala23		54.5	32.36		
Avi24		130.5	105.3		

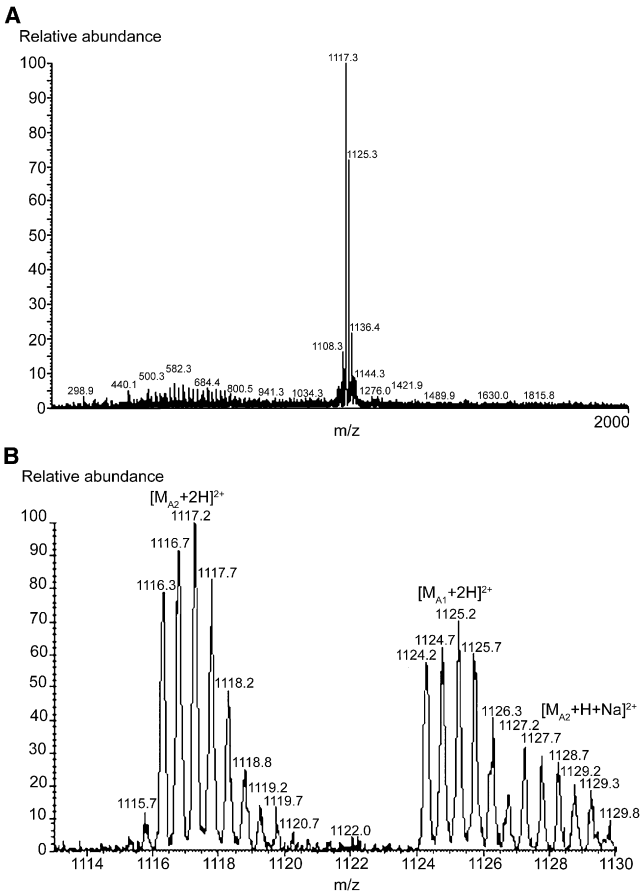

Figure 2. Mass Spectra of Microbisporicin A1 and A2 Obtained from Infusion Experiments

(A) Full-scan, low-resolution spectrum and (B) zoom-scan, high-resolution spectrum. Two doubly protonated ions $[M + 2H]^{2+}$ corresponding to microbisporicin A1 and A2 have *m/z* values at 1124 and at 1116 respectively. *M/z* at 1126 corresponded to the $[M_{A2} + H^+Na]^{2+}$ ion.

a molecular ion $[M + H]^+$ at *m/z* of 239. Tryptophan could not be detected in the hydrolysis mixture of microbisporicin A1 and A2.

The mass spectrum of the intact microbisporicin showed the presence of two intense signals at *m/z* of 1124 and 1116, corresponding to the double-charged ion $[M + 2H]^{2+}$ (Figure 2) of A1 and A2, respectively. In the full-scan spectrum range of 300–3000 mass units, the signals corresponding to the single-charged ions $[M + H]^+$ 2247 and 2231 were also present. The calculated molecular weights 2246 and 2230 Da were consistent with the assigned structures of A1 and A2.

Secondary Structure of Microbisporicin

We gained insight into the secondary structure of the antibiotic by analyzing the amide proton temperature coefficients, listed in Table 1 for microbisporicin A2, and solvent accessibility. Hydrogen bond formation typically stabilizes the exchangeable backbone amide protons and therefore reduces the exchange rate with the bulk solvent. Such stability can also be achieved when solvent accessibility is reduced as a result of steric constraints. Information about the extent to which hydrogens are bonded or sequestered from the solvent is gained by simply assessing the temperature dependency of the amide proton chemical shifts (Cierpicki and Otlewski, 2001; Hsu et al., 2003). A low dependency of the amide chemical shift on temperature in an aqueous environment (temperature coefficients, $\Delta\delta/\Delta t > -2.5$ ppb/K) is usually indicative of the presence of a stable hydrogen bond, while solvent-accessible amide protons are more sensitive to temperature change ($\Delta\delta/\Delta t < -5$ ppb/K). Based on the criteria listed above, stable amide protons with low solvent accessibility were identified for Ala21, Ala23, and Gly17, whereas Ala3, Ala20, and Phe22 were more strongly influenced by the solvent. In addition, the sequential NOEs used to assign the resonances (see Table S1) provided further evidence for regions of regular secondary structure in microbisporicin A2. The continuous stretch of medium-range sequential NN connectivities from residue Ala11 to Avi24 suggests that this region may adopt a compact rather than an extended conformation. In particular, the observed crosspeaks between residues Abu8-Phe22 and Pro9-Ala20 were indicative of a globular 3D structure of this region. In the case of microbisporicin A1, the presence of the 3,4-diOHPro in position 14 further increased the rigidity of the molecule. This was indicated by the slow conformational

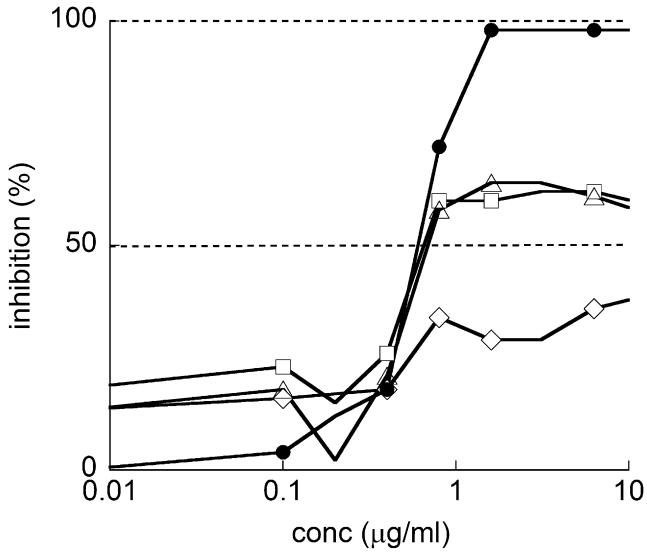

Figure 3. Inhibition Test of Macromolecular Syntheses in *Staphylococcus aureus*

Effect of microbisporicin on DNA (open diamonds), RNA (open squares), protein (open triangles), and PG syntheses (closed circles).

equilibrium in the solution of microbisporicin A1, which made it possible to distinguish and assign two separate conformers (Table S2). Further work is needed to determine the overall molecular conformations with distance constraints derived from NOESY experiments.

Mode of Action of Microbisporicin

Microbisporicin was active against *S. aureus* and inactive against its L forms that lacked a functional cell wall. The cell wall target was confirmed by testing the antibiotic in experiments of macromolecular syntheses in *S. aureus*. Figure 3 shows that PG biosynthesis was completely blocked by microbisporicin at a concentration of ~1 μg/ml. At this concentration, the effects on DNA, RNA, and protein syntheses were marginal. The inhibition patterns for microbisporicin were quite similar to those previously reported for glycopeptides and other lantibiotics, such as planosporicin and actagardine (Castiglione et al., 2007). However, planosporicin and actagardine blocked cell wall synthesis at higher concentrations of ~10 and 100 μg/ml, respectively. Indeed, lantibiotic nisin inhibited all macromolecular syntheses at the same concentration (~1 μg/ml), which is consistent with its disrupting action on membrane integrity (Castiglione et al., 2007).

The microbisporicin's mode of action was confirmed by the analysis of its effect on the cytoplasmic pool of UDP-linked PG precursors in *Bacillus megaterium.* When cells of *B. megaterium* were treated with microbisporicin, the cell wall precursor, uridinediphospho-N-acetylmuramyl-L-Ala-D-Glu-*m*Dap-D-Ala-D-Ala, accumulated in their hydrolyzates. This compound, which could not be detected in untreated cells, eluted with a retention time of 13.4 min in the LC-MS conditions described in the Experimental Procedures. Its positive and negative ion mode MS spectra and MS/MS fragmentation profile (data not shown) are identical to the ones that we previously reported for planosporicin- or vancomycin-treated cells (Castiglione et al., 2007). The accumulation of the UDP-MurNAc-pentapeptide is consistent with the data reported in a variety of bacteria treated with cell wall inhibitors acting at steps subsequent to its cytoplasmic synthesis, such as ramoplanin, vancomycin, teicoplanin, mannopeptimycins (Billot-Klein et al., 1997; Ruzin et al., 2004), and lantibiotics mersacidin and actagardine (Brotz et al., 1997, 1998a).

Antimicrobial Activity

Table 3 presents the spectrum of microbisporicin's antibacterial activity against a panel of important human pathogens. Individual factors A1 and A2 showed substantially identical activity against the entire panel (data not shown). Microbisporicin was active against major Gram-positive pathogens, including MRSA and vancomycin-resistant enterococci (VRE). Minimal inhibitory concentrations (MICs) were in the range of ≤ 0.13–4.0 μg/ml against *Staphylococci, Streptococci, Enterococci*, and *Lactobacilli*, indicating a potency comparable or superior to that of vancomycin and teicoplanin (French, 2006). The antibiotic was also very active against anaerobic *Clostridia* (MICs ≤ 0.13 μg/ml) and *Propionibacteria* (MICs ≤ 0.13–4 μg/ml). The activity of microbisporicin against aerobic and anaerobic Gram-positive bacteria appeared consistently superior with respect to the comparator lantibiotics planosporicin, actagardine, and mersacidin, and also with respect to the most active nisin. *Escherichia coli* or other enterobacteria were insensitive to lantibiotics. However, microbisporicin was more active than the comparators against the Gram-negative *Moraxella catarrhalis*, *Neisseria* spp., and *Haemophilus influenzae*. Consistent with the mode of action of cell wall inhibitors, no activity for microbisporicin was observed against *S. aureus* L form (L3751) and the eukaryote *Candida albicans*.

Efficacy in Animal Models

Antibiotic microbisporicin was tested against murine septicemia caused by *S. aureus* Smith 819 ATCC 19636 (MIC ≤ 0.13 μg/ml). Antibiotic microbisporicin protected mice with an antibiotic dose at 50% of in vivo efficacy (ED_{50}) of 2.1 mg/kg. This level of protection was observed both after intravenous (iv) and subcutaneous (sc) administration. In the same infection model, the reference drug, vancomycin (MIC = 0.5 μg/ml) showed an ED_{50} of 0.9 mg/kg by sc administration. Moreover, animals treated with high doses of microbisporicin (≥200 mg/kg) survived, thus indicating low acute toxicity either iv or sc.

DISCUSSION

This paper presents the novel and potent lantibiotic, microbisporicin. It was found through a screening process devised to discover selective PG synthesis inhibitors: (1) produced by uncommon actinomycetes; (2) essentially not cross-resistant with β-lactams and glycopeptides; and (3) effective against infections caused by Gram-positive pathogens. We found microbisporicin in a group of antibiotics that fulfilled these selection criteria.

The structure of microbisporicin is substantially different from any of the 50 previously described lantibiotics (Chatterjee et al., 2005; Jung, 2006). It was produced by an actinomycete species

Table 3. Antimicrobial Activity of Microbisporicin in Comparison to Planosporicin, Actagardine, Mersacidin, and Nisin

	Strain				
MIC (μg/ml)	Microbisporicin	Planosporicin	Actagardine	Mersacidin	Nisin
L100 *Staphylococcus aureus* ATCC6538P	≤0.13	2	32	4	0.5
L3751 *Staphylococcus aureus* L form	>128	>128	>128	64	16
L819 *Staphylococcus aureus* Smith ATCC19636	≤0.13	16	32	4	2
L1400 *Staphylococcus aureus* MRSA	≤0.13	16	16	8	2
L613 *Staphylococcus aureus* MRSA	≤0.13	32	16	64	8
L3798 *Staphylococcus aureus* VISA	2	128	128	128	32
L3797 *Staphylococcus aureus* VISA met-r	2	>128	>128	128	8
L3798 *Staphylococcus epidermidis* ATCC12228	≤0.13	32	128	16	2
L1729 *Staphylococcus haemolyticus* met-r	8	>128	>128	8	4
L49 *Streptococcus pyogenes*	≤0.13	0.5	2	n.d.	n.d.
L44 *Streptococcus pneumoniae*	≤0.13	4	32	4	0.25
L559 *Enterococcus faecalis*	1	16	32	32	4
L560 *Enterococcus faecalis* Van A	0.5	64	128	64	4
LA533 *Enterococcus faecalis* Van A	1	128	16	32	4
L568 *Enterococcus faecium*	2	64	64	64	2
L569 *Enterococcus faecium* Van A	1	128	128	64	2
LB518 *Enterococcus faecium* Van A	2	>128	>128	128	1
L884 *Lactobacillus garviae*	≤0.13	4	4	16	n.d.
L148 *Lactobacillus delbrueckii* ATCC04797	4	16	>128	>128	>128
L3607 *Clostridium perfringens* ATCC13124	≤0.125	≤0.25	4	8	≤0.13
L4018 *Clostridium difficile*	≤0.125	1	4	8	≤0.13
L4043 *Clostridium butyricum*	≤0.125	n.d.	n.d.	n.d.	n.d.
Propionibacterium granulosum ATCC25564	0.03	n.d.	n.d.	n.d.	n.d.
L1329 *Propionibacterium acnes*	0.5	n.d.	n.d.	n.d.	n.d.
Propionibacterium limphophylum ATCC27250	0.015	n.d.	n.d.	n.d.	n.d.
L970 *Haemophilus influenzae* ATCC19418	32	>128	>128	>128	>128
L76 *Moraxella catarrhalis* ATCC8176	0.25	1	32	2	1
L1613 *Neisseria meningitidis* ATCC13090	0.5	>128	>128	>128	8
L997 *Neisseria gonorrhoeae*	0.25	>128	>128	>128	4
L47 *Escherichia coli*	>128	>128	>128	n.d.	>128
L145 *Candida albicans*	>128	>128	>128	n.d.	>128

ATCC, American Type Culture Collection; met-r, methicillin-resistent; MIC, minimal inhibitory concentration; MRSA, methicillin-resistant *Staphylococcus aureus*; n.d., not detected; Van A, vancomycin-resistent; VISA, vancomycin-intermediate-resistent *Staphylococcus aureus*.
MICs were determined by broth microdilution assay (NCCLS, 1990) according to the procedure described in the Experimental Procedures.

of *Microbispora* as two structurally closely related components, A1 and A2, which differ in a hydroxylic group on the hydroxy-proline at position 14, and show an equal mode of action and antimicrobial spectrum. Microbisporicin A1 and A2 are peptides with a molecular weight of 2246 and 2230 Da, respectively. The 24-mer peptides are ribosomally synthesized and subsequently modified to introduce hydroxylated Pro and chlorinated Trp residues, which have never been detected in lantibiotics. Five thioether intramolecular bridges (a single Melan, three Lan, and the AviCys residue) are predictive of conformational constraints.

Indeed, NMR studies showed that the structure comprises a globular domain from Ala11 to Avi24, created by the formation of thioether bonds between residues Ala13 and Ala20 (ring C), Ala18 and Ala23 (ring D), and Ala21 and Cys24 terminal end (ring E). In this region, a certain degree of conformational flexibility was observed in the ring formed by the eight residues, Ala13–Ala20, where three sequential Gly are located. However, microbisporicin does not contain any conserved motif resembling the type B globular lantibiotic actagardine. A limited similarity with the globular lantibiotic mersacidin could be identified in the sequence of three Gly residues following Pro6 in mersacidin and 4-OH Pro14 in microbisporicin A2 (3,4-diOH Pro in A1), and between the C-terminal AviCys of microbisporicin and AviMeCys of mersacidin. In turn, the C-terminal ring of microbisporicin is nearly identical to the C-terminal AviCys in the type AI lantibiotics epidermin and gallidermin (Chatterjee et al., 2005;

Allgaier et al., 1986; Bonelli et al., 2006) and, to a lesser extent, in the type AII lantibiotic cypemycin (Chatterjee et al., 2005; Komiyama et al., 1993). The topology of the A, B, D, and E rings of microbisporicin is nearly identical to epidermin (Allgaier et al., 1986; Bonelli et al., 2006). Actually, the C ring is different and, in part, resembles that of ericin A, also a type AI lantibiotic (Chatterjee et al., 2005; Stein et al., 2002). Microbisporicin is similar to the recently discovered planosporicin (Castiglione et al., 2007) in the number of amino acid residues and intramolecular thioether bridges, but the amino acid composition and sequence and the positions of the five rings are definitively different. Only the N-terminal three amino acids (NH2-Val-Dhb-Ala) are similar to planosporicin (NH2-Ile-Dhb-Ala), which is in turn identical to nisin (Castiglione et al., 2007). Interestingly, the N-terminal portion of microbisporicin, from Val1 to Ala11, shows a great similarity in amino acid sequence and bridge formation with the N-terminal part of the linear type AI lantibiotics nisin, subtilin, epidermin, and gallidermin (Chatterjee et al., 2005; Cotter et al., 2005; Allgaier et al., 1986; Bonelli et al., 2006). This N-terminal sequence was found to be crucial for nisin and epidermin binding to the lipid II pyrophosphate region, as demonstrated by specific mutations drastically reducing antimicrobial activity (Brotz et al., 1998b; Hsu et al., 2004; Wiedemann et al., 2001). Moreover, the nisin binding to lipid II was antagonized by the N-terminal 1–12 fragment of nisin (Chan et al., 1996). It would be interesting to investigate whether the N-terminal region of microbisporicin has the same function as in nisin and epidermin. Microbisporicin contains an organic chlorine substituent at an aromatic ring, which is different from other lantibiotics. It is worth noting that other chemical classes of antibiotics acting on lipid II, such as glycopeptides and ramoplanin, contain a similar chlorine substituent on an aromatic ring, the lipophylic nature of which may contribute to their affinity for the membrane compartment (Parenti et al., 1990; Walsh, 2003).

Considering the mode of action, microbisporicin primarly blocked PG synthesis differently from nisin, which blocked all the principal macromolecular syntheses as a result of rapid cell membrane depolarization (Castiglione et al., 2007). Microbisporicin was active at concentrations significantly lower than those of mersacidin-actagardine-planosporicin lantibiotics and comparable to the effective concentrations of nisin. As previously reported for planosporicin and glycopeptides (Castiglione et al., 2007), microbisporicin caused accumulation of the cytoplasmic UDP-pentapeptide precursor of PG in growing bacterial cells. Such accumulation indicates that the multistep assembly of PG located at the membrane is inhibited; this has been observed in a series of antibiotics acting on this phase (Brotz et al., 1998a, 1997; Billot-Klein et al., 1997; Ruzin et al., 2004). The bactericidal activity of nisin has been generally found to be superior to other lantibiotics on the basis of MIC comparisons. Superior bactericidal activity has been explained by taking into account nisin's dual mechanism of action, mediated by lipid II binding and resulting in cell wall inhibition and pore formation (Breukink et al., 1999; Hasper et al., 2006). It has been recently reported that pore-forming capacity of the 22 amino acid long gallidermin and epidermin varies depending on the target strains, and that some microorganisms remain susceptible in spite of missing pore formation (Bonelli et al., 2006). It thus appears that the multiple activities may combine differently in lantibiotics. The discovery of microbisporicin, original in structure and specifically acting on the cell wall pathway, may provide additional insights into the molecular determinants of the biological activity of lipid II-targeting antibiotics.

Indeed, the spectrum of activity of microbisporicin covered important aerobic and anaerobic Gram-positive pathogens. MRSA and VRE were susceptible, which is consistent with the selection criteria applied in the original screening. The activity of microbisporicin appeared comparable to or better than those of reference antibiotics, such as vancomycin and teicoplanin (French, 2006). With respect to nisin, the spectrum of activity was comparable or enhanced. Microbisporicin showed activity against the Gram-negative bacteria *M. catarrhalis*, *Neisseria* spp., and *H. influentiae*, which were insensitive to most of the lantibiotics and moderately susceptible to nisin. The antibiotic showed good efficacy in vivo after a single administration in an experimental infection model caused by *S. aureus* in a mouse. ED_{50}s were identical after iv and sc administration. This may indicate that distribution and bioavailability are comparable between the two administration routes. These results, together with those that will be described elsewhere (P.C. et al., unpublished data) on the efficacy of microbisporicin in different animal models of infection, indicate that it is a promising antibacterial for the systemic treatment of serious nosocomial infections caused by multidrug-resistant pathogens.

SIGNIFICANCE

Microbisporicin, produced by an uncommon actinomycete and discovered in the course of a biological activity-guided screening for bacterial cell wall synthesis inhibitors others than β-lactams and glycopeptides, is the most potent antibacterial among the known lantibiotics. Its spectrum of activity covers most of the Gram-positive isolates of medical importance and some Gram-negative pathogens, which differs from other lantibiotics. Considering also its efficacy in vivo, microbisporicin represents a promising antibiotic. Its structure is substantially different from any other antibiotic described. Microbisporicin is produced as two structurally related and similarly active 24 amino acid-long polypeptides, containing two posttranslational modifications and five thioether intramolecular bridges. The sequences of the N-terminal and C-terminal portions of microbisporicin and the topology of A, B, D, and E rings show great similarity with the 22 amino acid-long lantibiotics epidermin and gallidermin. The 1–11 N-terminal sequence is very similar to that of nisin, which was found to be crucial for lantibiotic binding to the lipid II pyrophosphate region. It would be interesting to investigate whether the N-terminal region of microbisporicin has the same function and may account for its superior bactericidal activity in comparison with the other known lantibiotics. Microbisporicin's mode of action consists in the selective inhibition of bacterial cell wall synthesis. The discovery of this lantibiotic provides additional insights into the molecular determinants of the biological activity of lipid II-targeting antibiotics.

EXPERIMENTAL PROCEDURES

Bacterial Strains

B. megaterium ATCC 13632 and *S. aureus* 209 ATCC 6538P (L100) were purchased from the American Type Culture Collection (ATCC; Manassas VA). L-form cells were prepared (L3751) from L100 as previously described (Somma et al., 1977). *S. aureus* Smith 819 ATCC19636 and other clinical isolates were maintained in the Lepetit Culture Collection (L) at Vicuron Pharmaceuticals, Gerenzano, Italy. *Microbispora* sp., the producer of microbisporicin (initially patented as Antibiotic 107891 [Lazzarini et al., 2005]), was previously isolated in the Vicuron laboratory from a soil sample. It was deposited as *Microbispora* sp. ATCC PTA-5024 (ATCC).

Fermentation

Microbispora sp. ATCC PTA-5024 was cultivated at 30°C and then shaking this culture at 200 rpm in 500 ml Erlenmeyer flasks containing 100 ml of seed medium AF/MS (in g/l: dextrose, 20; yeast extract, 2; soybean meal, 8; NaCl, 1; and $CaCO_3$, 4; pH adjusted to 7.3), or in Chemap-Braun 20 l fermenters containing 15 l of the same medium, at 30°C and stirring at 600 rpm and 0.5 vvm (gas volume/liquid reactor volume/min) aeration. For fermentation, 300 l bioengineering fermenters were used that contained 200 l of the production medium, M8 (in g/l: starch, 20; glucose, 10; yeast extract, 2; hydrolyzed casein, 4; meat extract, 2; and $CaCO_3$, 3; pH adjusted to 7.0), inoculated with 7% preculture, at 28°C–30°C, stirred at 180 rpm, and aerated at 0.5 vvm. The production of microbisporicin was monitored by HPLC, as described below.

Isolation of Microbisporicin A1 and A2

Broth was harvested after 90–100 hours of fermentation and then filtered by tangential filtration (0.1 μm pore size membrane, Koch Carbo-Cor; Koch Membrane Systems, Inc.). The filtrate was stirred with 2.3% (v/v) Diaion HP 20 polystyrene resin (Mitsubishi Chemical Co.). The resin was then recovered, washed batch-wise with methanol:water (2:3, v/v), and eluted with methanol:*n*-butanol:water (9:1:1, v/v/v). The fractions containing the lantibiotic were pooled and concentrated under vacuum to a residue of raw material that was dissolved in *n*-butanol. This solution was extracted three times with water, reconcentrated under vacuum, and dissolved in petroleum ether. The antibiotic in the mycelium fraction was extracted by adding an equal volume of methanol, and was recovered accordingly after vacuum evaporation of the solvent. Crude antibiotic was purified by chromatography on an IST C8 70 × 460 mm column (EC; 40–70 μm particle size; 60 Å pore size; International Sorbent Technology), which was eluted by a Bùchi B-680 Medium Pressure Chromatography System with a 60 minute (25 ml/min flow rate) linear gradient from 20% to 60% of phase B (phase A: acetonitrile, 20 mM ammonium formate buffer [pH 6.6] 10:90 [v/v]); phase B: acetonitrile, 20 mM ammonium formate buffer [pH: 6.6], 90:10 [v/v]). The eluted fractions containing lantibiotics were pooled, concentrated, and lyophilized twice to generate a solid preparation of microbisporicin. Individual, pure A1 and A2 factors were obtained by preparative HPLC on a Symmetry Prep C18 Waters column (7 μm particle size, 7.8 × 300 mm). Microbisporicin A2 was purified by isocratic elution at a flow rate of 7 ml/min with 100 mM ammonium formate buffer (pH 4):acetonitrile (82.5:17.5, v/v). Microbisporicin A1 was purified by a 25 minute linear gradient elution from 30% to 45% of phase B (3.5 ml/min flow rate). Phase A was 25 mM ammonium formate buffer (pH 4.5):acetonitrile (95:5, v/v), and phase B was acetonitrile. The fractions from repeated chromatographic runs were pooled, concentrated under vacuum, and lyophilized sequentially three times to yield the purified factors as a white powder.

Analytical Chromatography

The fermentation and purification processes were monitored on a Waters HPLC instrument equipped with a Waters Symmetry Shield RP8 250 × 4.6 mm column, 5 μm particle size, and a Symmetry C_{18} (5 μm) 3.9 × 20 mm precolumn, both maintained at 50°C, and eluted at 1 ml/min flow rate according to the following multistep gradient program: 8 min at 30% phase B (acetonitrile) in phase A (acetonitrile:100 mM ammonium formate pH 4.5 buffer, 5:95 [v/v]), followed by a 20 minute linear gradient from 30% to 45%. Detection was at 282 nm. Microbisporicin A1 and A2 factors typically eluted after 16.3 and 16.8 minutes, respectively.

LC-MS and MS/MS Analyses

LC-MS and MS/MS experiments were performed with a ThermoQuest Finnigan LCQ Deca mass detector equipped with an ESI interface and Thermo Finnigan Surveyor MS pump, photo diode array detector (PDA) (UV6000; Thermo Finnigan), and an autosampler, as described previously (Meiring et al., 2002). The MS spectra were obtained by electrospray ionization, both in positive and negative mode, under the conditions described by Castiglione et al. (2007). In the infusion experiments, microbisporicin A1 or A2 was diluted to 0.1 mg/ml in water:acetonitrile (50:50, v/v) with 0.5% acetic acid (v/v). The ThermoQuest Finnigan LCQ Deca mass detector was previously tuned and calibrated in electrospray mode and used in infusion mode at 10 μl/min.

Hydrolysis and Amino Acid Analysis

Microbisporicin A1 or A2 (1 mg) was completely hydrolyzed by treatment for 24 hours in 6 N HCl at 105°C. The mixture of hydrolyzed amino acids was treated with N-hydroxysuccinimide-activated heterocyclic carbamate Waters AccQ-Fluor Reagent Kit (Pawlowska et al., 1993), and was then analyzed by LC-MS, as previously described by Castiglione et al. (2007). To determine the levels of 5-ClTrp, microbisporicin A1 or A2 (1 mg) was incubated for 16 hours in 0.6 ml of 4 N methanesulfonic acid containing 0.2% (w/v) 3-(2-aminoethyl)indole at 115°C, as described by Simpson et al. (1976). The hydrolysate, neutralized with 5 N NaOH and diluted in water, was analyzed by LC-MS. The separation was performed on a Waters Symmetry Shield C18 250 × 4.6 mm column, 5 μm particle size, equipped with a Symmetry C18 (5 μm) 3.9 × 20 mm precolumn and eluted at 1 ml/min flow rate with a 25 minute linear gradient from 0% to 50% of phase B (acetonitrile) in phase A (acetonitrile:25 mM ammonium formate [pH 4.5] buffer, 5:95 [v/v]). Detection was at 280 nm. The effluent from the column was split between PDA and MS detectors. The MS parameters were the same as described previously here, and the spectra were acquired in the 100 to 700 mass unit range. Under these conditions, standard samples of DL-tryptophan (Merck KGaA, Darmstadt, Germany) and 5-chloro-DL-tryptophan (Biosynt AG, Staad, Switzerland) typically eluted after 8.1 and 11.5 minutes, respectively, corresponding to $[M + H]^+$ at *m/z* 205 and 239, respectively.

NMR Spectroscopy

Microbisporicin dissolved poorly in water and showed some instability in dimethyl sulfoxide (DMSO). Therefore, the antibiotic was dissolved in a mixture of methanol/water acidified with drops of 0.01 N HCl. In these conditions, no degradation was observed when microbisporicin was incubated at temperatures ranging from 288K to 313K. NMR spectroscopic analyses were performed on the following samples: (1) 5.1 mg microbisporicin A1 factor dissolved in 0.6 ml of MeOH:d_3/H_2O (4:1, v/v); (2) 5.1 mg microbisporicin A2 dissolved in 0.6 ml of MeOH:d_3/H_2O (4:1, v/v.); and (3) 6 mg microbisporicin A2 dissolved in 0.6 ml CD_3CN:D_2O (1:1, v/v.). The following experiments were performed on all three samples: ^{1}H 1D spectrum, 2D DQF-COSY, TOCSY, and NOESY, with a watergate presaturation sequence, at 300K–290K. The NOESY experiment was conducted with a mixing time of 300 ms. 2D spectra were recorded with a spectral width of 12 ppm, 16 scans, 1024 T1-weighted increments, and 4096 T2-weighted complex data points. Heteronuclear ^{13}C-{^{1}H}, HSQC, and HMBC experiments were performed at 313K on sample 3. For the ^{13}C-{^{1}H} 1D spectrum, a sweep width of 220 ppm was used; 140K scans were accumulated, with a relaxation delay of 2 seconds. The HMQC and HMBC spectra were acquired with 1024 T1-weighted increments and 2048 T2-weighted complex data points, with a sweep width of 10 ppm in the proton and 220 ppm in the carbon dimension. These data were acquired on a Bruker AVANCE 750 MHz spectrometer equipped with a Z-gradient probe.

LC-MS Analyses of the Cytoplasmic PG Precursor Pool

B. megateriunm ATCC 13632 was cultivated in 100 ml Difco Mueller Hinton broth (MHB) at 37°C to an $A_{540\ nm}$ of 0.7. The culture was then divided into equal portions supplemented with antibiotic concentrations that were at least 100-fold greater than the MICs against *B. megaterium.* Vancomycin, teicoplanin, microbisporicin, planosporicin, and chloramphenicol were added at concentrations of 20, 20, 100, 100, and 100 μg/ml, respectively. The analysis of the cytoplasmic PG precursor pool was performed according to Kohlrausch and Holtje (1991). Briefly, after a 60 minute incubation at 37°C, the cells were

harvested, suspended in water (0.1 g fresh weight/ml) and boiled for 20 minutes. After cooling first at room temperature and then in ice, the suspension was then centrifuged at 39,000 × g for 30 minutes. The supernatant was lyophilized and dissolved in 0.1 volumes of water adjusted to pH 3 with formic acid. The samples were analyzed by reversed-phase HPLC and ESI-MS. Cytoplasmic PG precursors were separated on a C18 250 × 4.6 mm column (Phenomenex Luna), 5 μm particle size, eluted at a 1 ml/min flow rate with a 2 minute, 100% Phase A (2% acetonitrile:97.9% water:0.1% formic acid. v/v/v) and then a 50 minute linear gradient to 100% phase B (95% acetonitrile:4.915% water:0.085% formic acid, v/v/v). Column temperature was 22°C. The effluent from the column was split in a ratio of 1:5 between PDA and MS detectors, as described previously here.

Inhibition of Macromolecular Synthesis

S. aureus 209 ATCC 6538P (L100) was cultivated in Iso-Sensitest broth (ISS; Oxoid Ltd.) overnight at 37°C. The culture was then diluted 1:1 (v/v) in Davis Mingioli broth/ISS. At an $A_{540\ nm}$ of 0.4, macromolecular syntheses (DNA, RNA, protein, and PG) were monitored by incorporating the appropriate radioactive precursors: for DNA synthesis, [^{3}H]-thy (5 μCi/ml), with 0.1 g/l unlabeled adenosine; for RNA synthesis, [5,6 ^{3}H]-Ura (2 μCi/ml); for protein synthesis, L-[^{3}H]-leucine (10 μCi/ml); and for PG, N-acetyl-D-[1-^{3}H] glucosamine (1 μCi/ml), with 3.5 mg/l unlabeled N-acetylglucosamine. Of the resulting solutions, 100 μl were dispensed in 96-well microplates containing 10 μl of increasing concentrations of microbisporicin, planosporicin, teicoplanin, actagardine, or nisin. After 20 minutes of incubation at 37°C, 0.1 ml ice-cold 20% (w/v) trichloroacetic acid (TCA) was added to precipitate macromolecules. After 30 minutes at 4°C, the TCA precipitate was collected on glass fiber filters (Filtermat A; Wallac) with a 96-well cell harvester (Wallac), and radioactivity was determined in a β-plate scintillation counter (Wallac).

MIC Determinations

In vitro antimicrobial activity was determined by a broth microdilution assay, as recommended by the National Committee for Clinical Laboratory Standards (NCCLS, 1990). The growth media utilized to determine the MIC were: cation-adjusted Difco MHB for *Staphylococci*, *Enterococci*, *Bacilli*, *M. catarrhalis*, and *E. coli*; Todd Hewitt broth for *Streptococci*; *Lactobacilli* MRS broth (MRS) for *Lactobacilli*; GC medium plus 1% (v/v) Isovitalex plus 1% (v/v) hemine for *Neisseria*; Brain Hearth Infusion for *H. influentiae*; Brucella broth containing cysteine (0.5 g/l) for *Propionibacteria*; Wilkins Chalgren broth for *Clostridia*; and RPMI-1640 medium for *C. albicans.* Comparison of microbisporicin's activity versus *S. aureus* 209 ATCC 6538P (L100) and to its L form cells (L3751) was performed according to the cell wall assay described by Castiglione et al. (2007). Reversion of antimicrobial activity against *S. aureus* 209 ATCC 6538P (L100) was measured after adding β-lactamases coktail (Castiglione et al., 2007) or 2 mg/ml of ε-amino-caproyl-D-Ala-D-Ala, a glycopeptide affinity resin prepared as described previously (Corti et al., 1985).

Experimental Septicemia

Female outbred ICR (CD-1) mice (Harlan Italia) weighing 23–25 g were infected intraperitoneally with ~10^6 cells of *S. aureus* Smith 819 ATCC 19636 per mouse in 0.5 ml of bacteriological mucin (Difco). Microbisporicin was suspended in a medium composed of 10% DMSO (v/v), 10% (w/v) β-hydroxy-propyl cyclodextrin (Sigma), and 80% (v/v) of 5% (w/v) glucose in water at a final concentration from 5 to 10 mg/l. It was administered iv or sc within 10–15 minutes after infection. Vancomycin was used as the reference drug and was administered sc. The ED_{50} was calculated by the Spearman-Kärber method (Finney, 1952) from the percentage of animals surviving to the seventh day at each dose. A group of eight mice was treated for each experimental condition.

Supplemental Data

Supplemental Data, including three additional tables, are available with this article online at http://www.chembiol.com/cgi/content/full/15/1/22/DC1/.

ACKNOWLEDGMENTS

The authors thank Giancarlo Lancini for helpful discussions. The 750 MHz spectra were recorded at the SON NMR Large Scale Facility in Utrecht, which is funded by the European Union project "EU-NMR-European Network of Research Infrastructures for Providing Access & Technological Advancement in Bio-NMR" (FP-2005-RII3, contract 026145).

Received: August 25, 2007
Revised: October 16, 2007
Accepted: November 6, 2007
Published: January 25, 2008

REFERENCES

Allgaier, H., Jung, G., Werner, R.G., Schneider, U., and Zahner, H. (1986). Epidermin: sequencing of a heterodectic tetracyclic 21-peptide amide antibiotic. Eur. J. Biochem. *160*, 9–22.

Appelbaum, P.C. (2006). The emergence of vancomycin-intermediate and vancomycin-resistant *Staphylococcus aureus*. Clin. Microbiol. Infect. *12* (*Suppl 1*), 16–23.

Bax, A., and Davis, D.G. (1985). MLEV-17-based two-dimensional homonuclear magnetization transfer spectroscopy. J. Magn. Reson. *65*, 355–360.

Billot-Klein, D., Shlaes, D., Bryant, D., Bell, D., Legrand, R., Gutmann, L., and van Heijenoort, J. (1997). Presence of UDP-N-acetylmuramyl-hexapeptides and -heptapeptides in enterococci and staphylococci after treatment with ramoplanin, tunicamycin, or vancomycin. J. Bacteriol. *179*, 4684–4688.

Bonelli, R.R., Schneider, T., Sahl, H.G., and Wiedemann, I. (2006). Insights into in vivo activities of lantibiotics from gallidermin and epidermin mode-of-action studies. Antimicrob. Agents Chemother. *50*, 1449–1457.

Breukink, E., Wiedemann, I., van Kraaij, C., Kuipers, O.P., Sahl, H., and de Kruijff, B. (1999). Use of the cell wall precursor lipid II by a pore-forming peptide antibiotic. Science *286*, 2361–2364.

Brotz, H., Bierbaum, G., Reynolds, P.E., and Sahl, H.G. (1997). The lantibiotic mersacidin inhibits peptidoglycan biosynthesis at the level of transglycosylation. Eur. J. Biochem. *246*, 193–199.

Brotz, H., Bierbaum, G., Leopold, K., Reynolds, P.E., and Sahl, H.G. (1998a). The lantibiotic mersacidin inhibits peptidoglycan synthesis by targeting lipid II. Antimicrob. Agents Chemother. *42*, 154–160.

Brotz, H., Josten, M., Wiedemann, I., Schneider, U., Gotz, F., Bierbaum, G., and Sahl, H.G. (1998b). Role of lipid-bound peptidoglycan precursors in the formation of pores by nisin, epidermin and other lantibiotics. Mol. Microbiol. *30*, 317–327.

Castiglione, F., Cavaletti, L., Losi, D., Lazzarini, A., Carrano, L., Feroggio, M., Ciciliato, I., Corti, E., Candiani, G., Marinelli, F., and Selva, E. (2007). A novel lantibiotic acting on bacterial cell wall synthesis produced by the uncommon actinomycete *Planomonospora* sp. Biochemistry *46*, 5884–5895.

Chan, W.C., Leyland, M., Clark, J., Dodd, H.M., Lian, L.Y., Gasson, M.J., Bycroft, B.W., and Roberts, G.C. (1996). Structure-activity relationships in the peptide antibiotic nisin: antibacterial activity of fragments of nisin. FEBS Lett. *390*, 129–132.

Chatterjee, C., Paul, M., Xie, L., and van der Donk, W.A. (2005). Biosynthesis and mode of action of lantibiotics. Chem. Rev. *105*, 633–684.

Chatterjee, S., Chatterjee, D.K., Jani, R.H., Blumbach, J., Ganguli, B.N., Klesel, N., Limbert, M., and Seibert, G. (1992). Mersacidin, a new antibiotic from *Bacillus.* In vitro and in vivo antibacterial activity. J. Antibiot. (Tokyo) *45*, 839–845.

Cierpicki, T., and Otlewski, J. (2001). Amide proton temperature coefficients as hydrogen bond indicators in proteins. J. Biomol. NMR *21*, 249–261.

Corti, A., Rurali, C., Borghi, A., and Cassani, G. (1985). Solid-phase enzyme-receptor assay (SPERA): a competitive-binding assay for glycopeptide antibiotics of the vancomycin class. Clin. Chem. *31*, 1606–1610.

Cotter, P.D., Hill, C., and Ross, R.P. (2005). Bacterial lantibiotics: strategies to improve therapeutic potential. Curr. Protein Pept. Sci. *6*, 61–75.

Finney, D.J. (1952). The Spearman -Kärber method. In Statistical Methods in Biological Assay (London, England: Charles Griffin &Co, Ltd), pp. 524–530.

French, G.L. (2006). Bactericidal agents in the treatment of MRSA infections—the potential role of daptomycin. J. Antimicrob. Chemother. *58*, 1107–1117.

Griesinger, C., Otting, G., Wüthrich, K., and Ernst, R.R. (1988). Clean TOCSY for 1H spin system identification in macromolecules. J. Am. Chem. Soc. *110*, 7870–7872.

Hasper, H.E., Kramer, N.E., Smith, J.L., Hillman, J.D., Zachariah, C., Kuipers, O.P., de Kruijff, B., and Breukink, E. (2006). An alternative bactericidal mechanism of action for lantibiotic peptides that target lipid II. Science *313*, 1636–1637.

Hsu, S.T., Breukink, E., Bierbaum, G., Sahl, H.G., de Kruijff, B., Kaptein, R., van Nuland, N.A., and Bonvin, A.M. (2003). NMR study of mersacidin and lipid II interaction in dodecylphosphocholine micelles. Conformational changes are a key to antimicrobial activity. J. Biol. Chem. *278*, 13110–13117.

Hsu, S.T., Breukink, E., Tischenko, E., Lutters, M.A., de Kruijff, B., Kaptein, R., Bonvin, A.M., and van Nuland, N.A. (2004). The nisin-lipid II complex reveals a pyrophosphate cage that provides a blueprint for novel antibiotics. Nat. Struct. Mol. Biol. *11*, 963–967.

Johnson, A.P., and Woodford, N. (2002). Glycopeptide-resistant *Staphylococcus aureus*. J. Antimicrob. Chemother. *50*, 621–623.

Jung, G. (1991). Lantibiotics—a survey. In Nisin and Novel Lantibiotics, G. Jung and H.G. Sahl, eds. (Leiden, the Netherlands: ESCOM), pp. 1–34.

Jung, G. (2006). Enzyme-catalyzed sulfide ring formation in lantibiotics. Angew. Chem. Int. Ed. Engl. *45*, 5919–5921.

Kohlrausch, U., and Holtje, J.V. (1991). One-step purification procedure for UDP-N-acetylmuramyl-peptide murein precursors from *Bacillus cereus*. FEMS Microbiol. Lett. *62*, 253–257.

Komiyama, K., Otoguro, K., Segawa, T., Shiomi, K., Yang, H., Takahashi, Y., Hayashi, M., Otani, T., and Omura, S. (1993). A new antibiotic, cypemycin. Taxonomy, fermentation, isolation and biological characteristics. J. Antibiot. (Tokyo) *46*, 1666–1671.

Lazzarini, A., Cavaletti, L., Toppo, G., and Marinelli, F. (2001). Rare genera of actinomycetes as potential producers of new antibiotics. Antonie Van Leeuwenhoek *79*, 399–405.

Lazzarini, A., Gastaldo, L., Candiani, P., Ciciliato, I., Losi, D., Marinelli, F., Selva, E., and Parenti, F. (2005). Antibiotics 107891, its factors A1 and A2, pharmaceutically acceptable salts and compositions, and use thereof. International Publication Number WO 2005/014628 A, International Publication Date 17 February 2005.

Machaidze, G., and Seelig, J. (2003). Specific binding of cinnamycin (Ro 09–0198) to phosphatidylethanolamine. Comparison between micellar and membrane environments. Biochemistry *42*, 12570–12576.

Meiring, H.D., Van der Heeft, E., Ten Hove, G.J., and de Jong, A.P.J. (2002). Nanoscale LC-MS(n): technical design and applications to peptide and protein analysis. J. Sep. Sci. *25*, 557–568.

National Committee for Clinical Laboratory Standards (1990). Approved Standard M7-A2: Methods for Dilution Antimicrobial Susceptibility Testing for Bacteria that Grow Anaerobically, Second Edition Approved Standard M7-A2. (Villanova, PA: NCCLS).

Pag, U., and Sahl, H.G. (2002). Multiple activities in lantibiotics—models for the design of novel antibiotics? Curr. Pharm. Des. *8*, 815–833.

Parenti, F., Ciabatti, R., Cavalleri, B., and Kettenring, J. (1990). Ramoplanin: a review of its discovery and its chemistry. Drugs Exp. Clin. Res. *16*, 451–455.

Parenti, F., Pagani, H., and Beretta, G. (1976). Gardimycin, a new antibiotic from *Actinoplanes*. I. Description of the producer strain and fermentation studies. J. Antibiot. (Tokyo) *29*, 501–506.

Pawlowska, M., Chen, S., and Armstrong, D.W. (1993). Enantiomeric separation of fluorescent, 6-aminoquinolyl-N-hydroxysuccinimidyl carbamate, tagged amino acids. J. Chromatogr. *641*, 257–265.

Ruzin, A., Singh, G., Severin, A., Yang, Y., Dushin, R.G., Sutherland, A.G., Minnick, A., Greenstein, M., May, M.K., Shlaes, D.M., and Bradford, P.A. (2004). Mechanism of action of the mannopeptimycins, a novel class of glycopeptide antibiotics active against vancomycin-resistant gram-positive bacteria. Antimicrob. Agents Chemother. *48*, 728–738.

Simpson, R.J., Neuberger, M.R., and Liu, T.Y. (1976). Complete amino acid analysis of proteins from a single hydrolysate. J. Biol. Chem. *251*, 1936–1940.

Somma, S., Merati, W., and Parenti, F. (1977). Gardimycin, a new antibiotic inhibiting peptidoglycan synthesis. Antimicrob. Agents Chemother. *11*, 396–401.

Stein, T., Borchert, S., Conrad, B., Feesche, J., Hofemeister, B., Hofemeister, J., and Entian, K.D. (2002). Two different lantibiotic-like peptides originate from the ericin gene cluster of *Bacillus subtilis* A1/3. J. Bacteriol. *184*, 1703–1711.

Walsh, C. (2003). Antibiotics that block cell wall biosynthesis. In Antibiotics, Actions, Origins, Resistance, C. Walsh, ed. (Washington, D.C.: ASM Press), pp. 23–49.

Wiedemann, I., Breukink, E., van Kraaij, C., Kuipers, O.P., Bierbaum, G., de Kruijff, B., and Sahl, H.G. (2001). Specific binding of nisin to the peptidoglycan precursor lipid II combines pore formation and inhibition of cell wall biosynthesis for potent antibiotic activity. J. Biol. Chem. *276*, 1772–1779.

Wishart, D.S., and Nip, A.M. (1998). Protein chemical shift analysis: a practical guide. Biochem. Cell Biol. *76*, 153–163.

Wüthrich, K. (1986). NMR of proteins and nucleic acids (New York: Wiley).